JJEES

JJEES (2025) 16 (3): 267-275
ISSN 1995-6681

Jordan Journal of Earth and Environmental Sciences

# Assessing Land Use/Land Cover and Predicting Future Scenarios in Kano Metropolis, Northern Nigeria

Akus Kingsley Okoduwa[1*], Chika Floyd Amaechi[1] , Alex Ajeh Enuneku[1,2]

[1] Department of Environmental Management and Toxicology, Faculty of Life Sciences, University of Benin, PMB 1154, Benin City, Nigeria.
[2] Laboratory for Ecotoxicology and Environmental Forensics, University of Benin, PMB 1154, Benin City, Nigeria

Received on August 26, 2024, Accepted on February 22, 2025

**Abstract**

Uncontrolled urban development has significant implications for sustainable urban progress. Assessing and predicting changes in land use/land cover (LULC) are essential for effective environmental monitoring and management. This study evaluates LULC changes from 1984 - 2023 in the Kano metropolis, Nigeria, while also forecasting future transformations. Landsat-5 Thematic Mapper (1984), Landsat-4 Thematic Mapper (1998), and Landsat-8 Operational Land Imager/Thermal Infrared Sensor (2023) imagery from the United States Geological Survey Earth Explorer were used. LULC classification was conducted using the support vector machine (SVM) supervised approach, categorizing the landscape into built-up areas, vegetation, water bodies, and bare land. The accuracy of the classified LULC maps was computed using ENVI 5.3, ArcGIS, and Google Earth Pro. The CA-Markov model in IDRISI TerrSet Software (2020) was employed to project LULC changes for 2050. The classification accuracies for 1984, 1998, and 2023 were 99.59%, 94%, and 98.96%, respectively, with kappa coefficients of 0.99, 0.92, and 0.98. The results indicate a 41.8% increase (204.63 km²) in built-up areas from 1984 - 2023, while vegetation expanded by 2% (8.55 km²). Water bodies slightly decreased by 0.12 km² (<1%), and bare land declined by 213.35 km² (43%). Projections for 2050 anticipate further expansion of built-up areas (16%) alongside reductions in vegetation (1%), water bodies (<1%), and bare land (16%). These findings suggest continued urban growth at the expense of natural landscapes. To enhance environmental sustainability, this study recommends ecosystem-based adaptation strategies and legal frameworks to mitigate the adverse effects of urban expansion.



**Keywords:** *LULC, CA-Markov model, Projection, Kano Metropolis, Nigeria*

## 1. Introduction

According to Bren d'Amour et al. (2016) findings, global urbanization by 2030 will cause arable land losses of 1.8 to 2.5%, with Africa and Asia accounting for 80% of this loss. Given that more than 60% of the world's irrigation fields are near urban areas, there is potential competition for land between agriculture and urbanization (Mohammad, 2020). By 2050, more than 68% of the world's population, approximately 9.8 billion people, will reside in cities, with the majority residing in less-developed countries (Li et al., 2013; United Nations, 2020). This demographic shift will impose considerable pressure on resource consumption, especially in terms of land-use changes (Alqahtany et al., 2013), potentially leading to uncontrolled urban sprawl (Osman et al., 2018) and significant alterations in the urban-regional landscape (Xu et al., 2012).

The rapid urbanization and growth rate in Kano, Nigeria, pose substantial challenges to urban environmental sustainability. Kano's urbanization has made it Nigeria's most populous northern urban state (Okopi, 2021). Urbanization attracts populations, shapes activities, and drives infrastructure development, including road networks, public utilities, and land-use changes (Mohammad, 2020), leading to expanded built-up areas, diminished green spaces, increased urban surface temperatures, urban heat island formation, and climate change (Singh et al., 2017; Wang, 2019; Huang et al., 2019; Rigden and Li, 2017; Li et al., 2018; Liang et al., 2019; Fabolude and Aighewi, 2022; Amaechi et al., 2023, Okoduwa et al., 2024).

Analyzing land-use changes across past, present, and future scenarios allows for assessing resource expansion and degradation, guiding current and prospective land-use decisions (Mohammad, 2020). Furthermore, understanding the impact of urban development informs the adoption of efficient land management policies and strategies (Nourqolipour et al., 2016; Munthali et al., 2019). Addressing urban challenges requires enhancing urban land-use efficiency for sustainable development (Zhu et al., 2019) and analysing the root causes of uncontrolled urban growth for improved future planning (Osman, 2018).

Modelling LULC changes offers an effective way to simulate land-use dynamics and understand interactions between LULC changes and the environment (Lia et al., 2016; Tobore et al., 2021). Various methods exist for modeling LULC changes, including Cellular Automata (CA) (He et al., 2005), Clue-s model (Verburg and Overmars, 2007), Markov model (Guan et al., 2008), and the hybrid CA-Markov model (Khawaldah, 2016). The Markov model is widely used for simulating and predicting LULC changes, indicating change directions and providing a framework for assessing future land-use demands (Jiansheng et al., 2012). However, traditional models often lack spatial analysis capabilities and

* Corresponding author e-mail: okoduwaakus@gmail.com

struggle to predict land requirements within geographical space (Han et al., 2015). In contrast, the CA-Markov model offers robust dynamic simulation capabilities, effectively representing spatial and temporal changes by combining the strengths of both the Markov and CA models (Yuan et al., 2015).

By integrating the spatial continuity of the cellular automata (CA) model with the Markov chain's long-term prediction abilities, the CA-Markov hybrid model has proven effective for modeling various LULC classes (Chotchaiwong and Wijitkosum, 2019). This hybrid approach offers a dynamic, reliable, and robust technique for predicting spatiotemporal LULC changes in rapidly developing urban areas. Several studies (Liping et al., 2018; Wang et al., 2018; Sun et al., 2018; Samat et al., 2020; Wang et al., 2022; Fabolude and Aighewi, 2022; and Amaechi et al., 2023) have demonstrated the effectiveness of the CA-Markov model in predicting LULC change. Using this hybrid model as a predictive tool can significantly contribute to effective land use planning, management, and ecological system restoration (Koko et al., 2022).

This study addresses the critical gap in understanding the long-term impact of urbanization on LULC dynamics in Kano Metropolis. While previous research has examined urban growth in Nigeria, limited studies have provided a spatiotemporal assessment covering nearly four decades (1984–2023). Additionally, the lack of predictive models for future urban expansion has hindered proactive urban planning. By employing the CA-Markov model, this study projects LULC changes for 2050, offering a data-driven approach to inform sustainable land management policies. The findings contribute to knowledge by providing evidence of urban expansion trends, their implications for environmental sustainability, and the need for adaptive urban planning strategies in rapidly growing cities like Kano.

## 2. Materials and methods

### 2.1. Study area

Kano Metropolis (Figure 1) is located between latitudes 11°51'0'N and 12°01'30'N and longitudes 8°25'0'E to 8°30'0'E. It is located in northern Nigeria's most populous state, and the study area is Nigeria's second most populous metropolis (Koko et al., 2022). The city's urban population was 3.8 million in 2018, and it is predicted to grow to 5.6 million by 2030 (Koko et al., 2022). Kano's urban structure has evolved, with significant transformations driven by industrialization and economic development in the 21st century. The city's urban fabric has gradually been shaped by rapid urban expansion, extending from the central and densely settled zones to the peripheral and surrounding areas of the urban center (Mohammed et al., 2014).

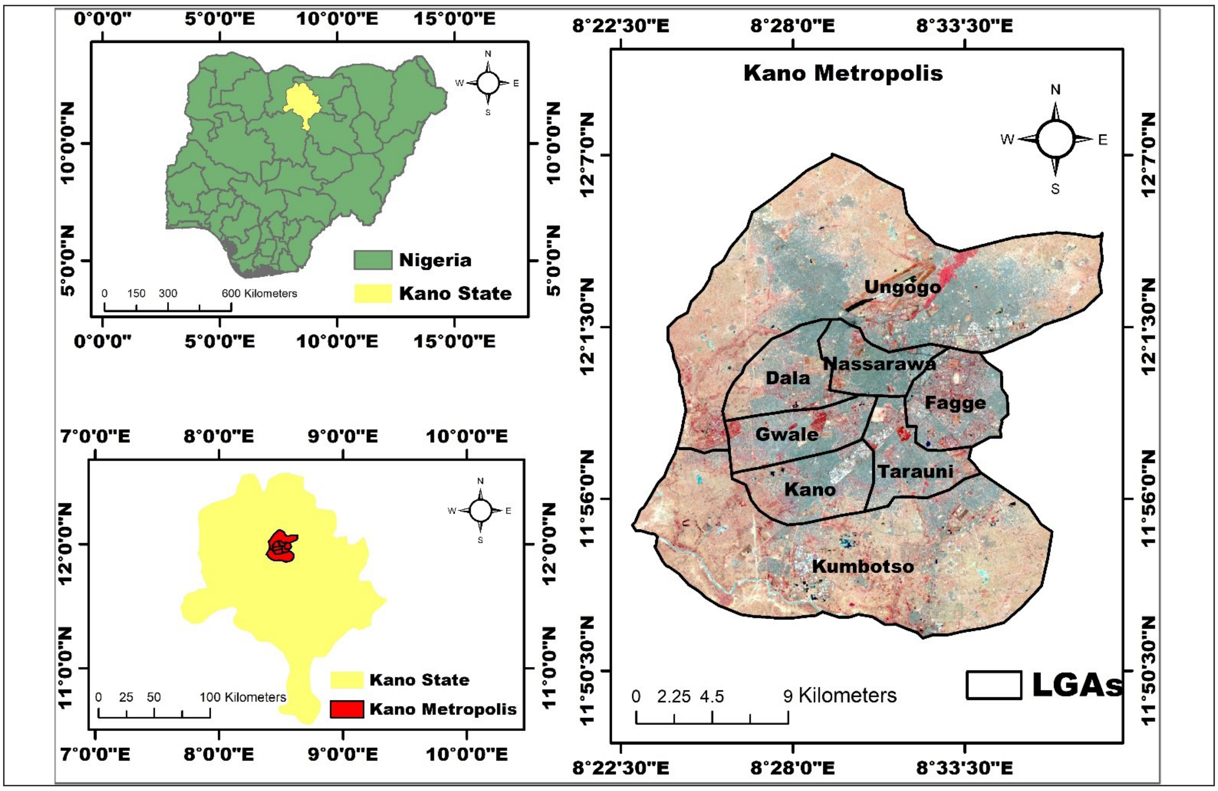

**Figure 1.** Study area (Kano Metropolis) displayed using a False Color Composite with Landsat 8 bands 5 (Near Infrared), 4 (Red), and 3 (Green) to enhance land cover distinction.

The city has a wet season that lasts from May to October, followed by a dry season from November to April (Dankani, 2013). The annual precipitation in Kano varies between its northern and southern regions, from 800 mm to 1100 mm (Nabegu, 2014). The city's average yearly temperature is approximately 26°C (Nwagbara, 2015). Kano has an abundance of fertile soil that supports a variety of food and cash crops, including millet, rice, sorghum, wheat, cowpeas, groundnuts, and other vegetables (Koko et al., 2022). The metropolis is one of Nigeria's fastest-growing urban areas, and its commercial and agricultural activities have continued to attract new residents (Okopi, 2021).

### 2.2 Data Acquisition

This study utilized Landsat 5 Thematic Mapper (TM), Landsat 4 Thematic Mapper (TM), and Landsat 8 Operational Land Imager/Thermal Infrared Sensor (OLI/TIRS) data for path and row 188/054 from 1984, 1998, and 2023 (Table 1). These images were obtained from the United States Geological Survey (USGS) website (https://earthexplorer.usgs.gov/). To ensure data quality and enhance the reliability of the analyses, only images with 0.00% cloud cover were selected.

The selection of Landsat 5 for 1984 and Landsat 4 for 1998 was based on image availability with 0.00% cloud cover. While both satellites carried the TM sensor, Landsat 5 was chosen for 1984 because it provided a cloud-free image for that year. For 1998, the cloud-free image available came from Landsat 4, making it the most suitable option for maintaining consistency in data quality. Thus, the choice of data sources was guided by the need to ensure the highest quality cloud-free imagery for analysis.

**Table 1.** Data type and data sources

| Data | Source | Resolution | Land/Scene Cloud Cover | Date |
|---|---|---|---|---|
| Landsat 5 TM | USGS Earth Explorer | 30 | 0.00 | 1984-12-29 |
| Landsat 4 TM | USGS Earth Explorer | 30 | 0.00 | 1998-11-18 |
| Landsat 8 OLI/TIRS | USGS Earth Explorer | 30 | 0.00 | 2023-12-09 |

### 2.3 Image Preprocessing

To ensure the accuracy and reliability of the classification results, preprocessing was performed on the Landsat images before classification. ENVI (Environment for Visualizing Images) software version 5.3 was used for image preprocessing, which included radiometric calibration, atmospheric correction, geometric correction, and clipping of the study area.

Radiometric Calibration: This step converted the digital numbers (DN) of the Landsat images into at-sensor radiance values, correcting for sensor-specific variations and ensuring consistency across different acquisition years.

Atmospheric Correction: Atmospheric correction was performed using the Fast Line-of-Sight Atmospheric Analysis of Spectral Hypercubes (FLAASH) tool in ENVI 5.3. FLAASH removes the effects of atmospheric scattering and absorption, thereby enhancing the spectral fidelity of the images and improving the accuracy of land cover classification.

Geometric Correction: The images were georeferenced to the Universal Transverse Mercator (UTM) coordinate system using the World Geodetic System (WGS) 1984 datum to ensure spatial alignment across different years. This correction minimizes geometric distortions caused by variations in satellite positioning and terrain effects.

Clipping of the Study Area: To focus on the region of interest, each Landsat image was clipped to the boundaries of Kano Metropolis using a shapefile of the study area. This step eliminated unnecessary data outside the study area, reducing processing time and improving classification accuracy. These preprocessing steps were essential for ensuring data consistency, reducing atmospheric and radiometric distortions, and enhancing the accuracy of subsequent classification and analysis.

### 2.4 Image Classification

ENVI software version 5.3 was utilized for LULC classification of the 1984 and 2023 images, while ArcGIS 10.7.1 was used for the 1998 image. A limitation of the cracked version of ENVI is the lack of support for Landsat 4 data processing. Consequently, ArcGIS was selected to effectively process and classify the 1998 image while maintaining overall methodological consistency. Despite the use of different software, classification consistency was ensured by applying the same supervised classification approach and validation techniques across all datasets. The same algorithm (SVM) was used to classify all land cover classes.

Implementing this technique on Landsat images included utilizing four distinct classes: built-up (impervious surface area including building materials and asphalt), vegetation (areas dominated by trees and grasses), waterbody (area covered by water), and bare land (non-vegetated barren areas) (Okoduwa and Amaechi, 2024). These land cover classes were selected for this study based on the observed land cover classes available within the Landsat images through false and true color composites. The supervised classification process involved the use of meticulously collected training signature samples. The CA-Markov model in TerrSet Geospatial Monitoring and Modelling Software version 2020 was utilized to carry out LULC projections for 2050. ArcGIS 10.7.1 was used to mask the boundaries of the study area, perform post-classification operations, generate statistical data, develop map layouts, and create visualizations. Figure 2 depicts the research methodology flowchart.

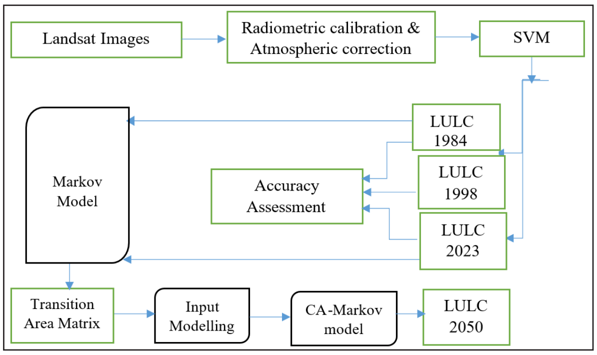


**Figure 2.** Research methodology flowchart for LULC classification and projection

### 2.5 Accuracy Assessment

The accuracy assessment of the classified LULC maps was conducted using different methodologies, reflecting the software used for classification. ENVI 5.3 was utilized for the accuracy assessment of the 1984 and 2023 images, while ArcGIS and Google Earth Pro were used for the 1998 image. This approach was necessary to maintain methodological consistency, as ENVI was used for classifying the 1984 and 2023 images, whereas ArcGIS was used for the classification of the 1998 image. Additionally, Google Earth Pro provided access to historical high-resolution imagery, which enhanced the validation process for 1998.

In ENVI 5.3, accuracy assessment was performed through a two-step process. First, various band combinations were used to extract ground truth pixels from high-resolution raster images (unclassified rasters) for 1984 and 2023, representing distinct land cover classes. Next, the polygon tool was employed to extract corresponding ground truth pixels from the classified maps for these years. The Ground Truth ROI function in ENVI 5.3 was then used to generate a confusion matrix, comparing the classified land cover pixels with the reference ground truth data. The results, including the number of correctly and incorrectly classified pixels, are presented in Tables 2 and 4.

For the 1998 image, an accuracy assessment was conducted using ArcGIS and Google Earth Pro. A total of 100 accuracy assessment points were generated in ArcGIS using the Create Accuracy Assessment Points tool, with the equalized stratified random sampling method ensuring balanced distribution across all LULC classes. The generated points were then converted to KML format and imported into Google Earth Pro, where the Show Historical Imagery feature was used to retrieve corresponding 1998 satellite imagery (Figure 3). Each assessment point was visually cross-referenced with the historical imagery to verify classification accuracy.

Following validation, a confusion matrix was computed in ArcGIS to assess classification performance. The overall accuracy, 'user's accuracy (UA), 'producer's accuracy (PA), and Kappa coefficient (KC) were then derived to quantify classification reliability, as presented in Equation 1-4. Table 3 shows the numbers of correct and incorrect ground truth points for 1998.

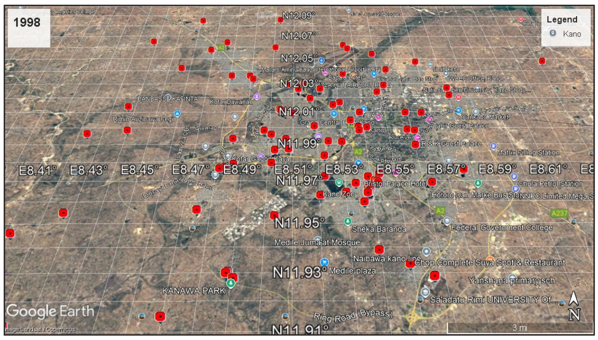


**Figure 3.** Google Earth Pro showing 1998 image for accuracy assessment.

**Table 2.** Correct and incorrect numbers of ground truth pixels for 1984

| LULC Class | Built-up | Vegetation | Waterbody | Bareland | Total |
|---|---|---|---|---|---|
| Built-up | 1418 | 0 | 12 | 4 | 1434 |
| Vegetation | 1 | 286 | 5 | 2 | 294 |
| Water bodies | 1 | 0 | 97 | 0 | 98 |
| Bareland | 2 | 6 | 4 | 7105 | 7117 |
| Total | 1422 | 292 | 118 | 7111 | 8943 |

**Table 3.** Correct and incorrect numbers of ground truth points for 1998

| LULC Class | Built-up | Vegetation | Water bodies | Bare land | Total |
|---|---|---|---|---|---|
| Built-up | 1 | 22 | 0 | 2 | 25 |
| Vegetation | 22 | 0 | 0 | 3 | 25 |
| Water bodies | 0 | 0 | 25 | 0 | 25 |
| Bare land | 0 | 0 | 0 | 25 | 25 |
| Total | 23 | 22 | 25 | 30 | 100 |

**Table 4.** Correct and incorrect numbers of ground truth pixels for 2023

| LULC Class | Built-up | Vegetation | Waterbody | Bareland | Total |
|---|---|---|---|---|---|
| Built-up | 5900 | 1 | 40 | 7 | 5948 |
| Vegetation | 0 | 282 | 0 | 3 | 285 |
| Water bodies | 0 | 0 | 321 | 0 | 321 |
| Bareland | 22 | 15 | 2 | 2063 | 2102 |
| Total | 5922 | 298 | 363 | 2073 | 8656 |

The various accuracy assessments can be calculated using the following formulas:

$$\text{Consumer Accuracy} \; \frac{\text{Number of correctly classified training samples in each class}}{\text{Number of training samples classified to that class}} \quad (1)$$

$$\text{Producer Accuracy} \; \frac{\text{Number of correctly classified training samples in each class}}{\text{Number of training samples in each class}} \quad (2)$$

$$\text{Overall Accuracy} = \frac{\text{Number of correctly trained samples}}{\text{Number of total samples}} \quad (3)$$

$$\text{Koppa coefficient} = \frac{\text{Overall Accuracy} - \text{Estimated chance agreement}}{1 - \text{Estimated chance of agreement}} \quad (4)$$

(Nasiri et al., 2022; Kadri et al., 2023, Okoduwa & Amaechi, 2024)

## 3. Results

### *3.1 Accuracy Assessment*

Table 5 presents the classification accuracy for 1984, 1998, and 2023. The overall accuracies for the three years (1984, 1998, and 2023) were 99.59%, 94, and 98.96%, respectively. The kappa coefficients were 0.99, 0.92, and 0.98, respectively, which are considered acceptable (Tadese et al., 2020; Koko et al., 2022; Amaechi et al., 2024).

**Table 5**. Accuracy assessment results for 1984, 1991, and 2023

| Class | 1984 | | 1991 | | 2023 | |
|---|---|---|---|---|---|---|
| | PA | UA | PA | UA | PA | UA |
| Build-up | 99.72 | 98.88 | 0.96 | 0.88 | 99.63 | 99.19 |
| Vegetation | 97.95 | 97.28 | 100 | 0.88 | 94.63 | 98.95 |
| Water bodies | 82.20 | 98.98 | 100 | 100 | 88.43 | 100 |
| Bareland | 99.92 | 99.83 | 0.83 | 100 | 99.52 | 98.14 |
| Overall Accuracy | **99.59** | | **94** | | **98.96** | |
| Koppa Coefficient | **0.99** | | **0.92** | | **0.98** | |

### *3.2 Spatial distribution of LULC*

The findings of the geospatial evaluation for the year 1984 (Figure 4) demonstrate a landscape that has yet to experience significant change from anthropogenic activities, as evidenced by the quantity of vegetation in the Fagge local government area. The built-up class was concentrated in Nassarawa and the southern part of Ungogo. Tarauni, Kano, Gwale, Dala, and Kumbotso were covered with bare land. The assessment results for the year 1998 (Figure 5) show that built-up area is gradually increasing, and bare land and water bodies are being lost within Fagge, Ungogo, and Nassarawa. Increased patches of vegetation were found in Tarauni.

The assessment results for the year 2023 (Figure 6) show that vegetation and bare land are gradually being lost over time and replaced with built-up areas within Fagge, Tarauni, Ungogo, Kano, Gwale, Dala, and Kumbotso. Some patches of vegetation were also found across the eight local government areas (LGAs). The projected year (Figure 7) reveals a massive built-up area within all the respective local government areas of the Kano metropolis. Some patches of vegetation are still projected to occur within the six LGAs. By 2050, the built-up area is expected to increase by approximately 82.89 km², representing a 16% growth from 2023 levels. This continued urban expansion suggests that previously undeveloped land will be converted to residential, commercial, and industrial uses, reflecting population growth and economic development pressures. Expanding urban areas could have profound implications for environmental sustainability, including increased land surface temperature, heightened pollution levels, and greater demand for infrastructure and public services.

Vegetation cover, on the other hand, is projected to decline by 4.7 km² (1%), indicating the ongoing loss of green spaces due to urban encroachment. This reduction in vegetation could lead to adverse ecological consequences, such as decreased air quality, disruption of local climate regulation, and the exacerbation of the urban heat island effect. Similarly, bare land is expected to decrease by 78.13 km² (16%) as more open spaces are converted to built-up areas. The rapid decline in bare land signifies the increasing pressure on available land resources, necessitating effective land-use policies to balance development with environmental conservation. In contrast, water bodies are projected to remain relatively stable, with a minimal decrease of 0.06 km². While this suggests that urban expansion may have a limited direct impact on water bodies, indirect effects such as pollution and increased water demand could pose challenges for water resource management in the long term.

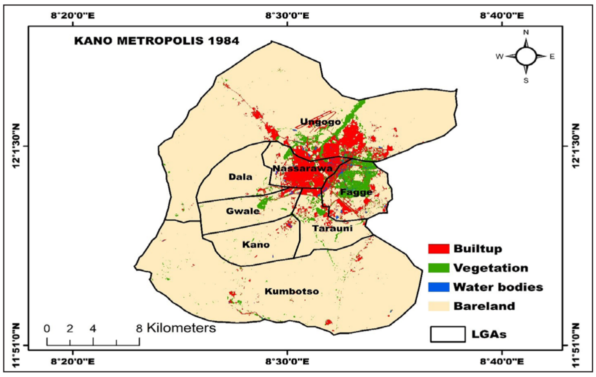


**Figure 4.** LULC map of 1984

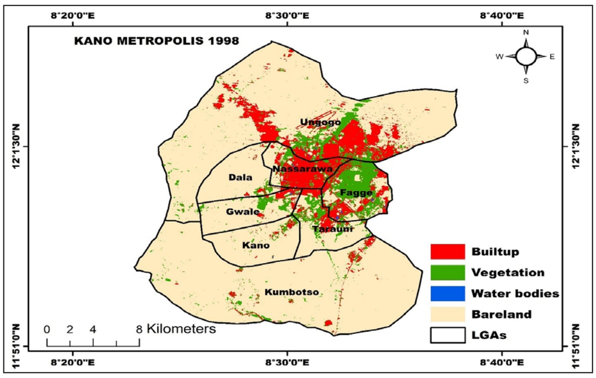


**Figure 5.** LULC map of 1998

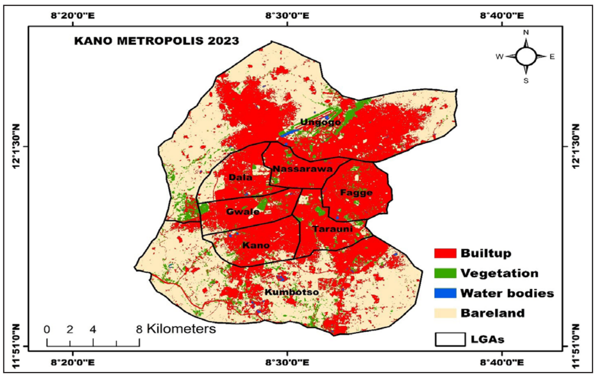


**Figure 6.** LULC map of 2023

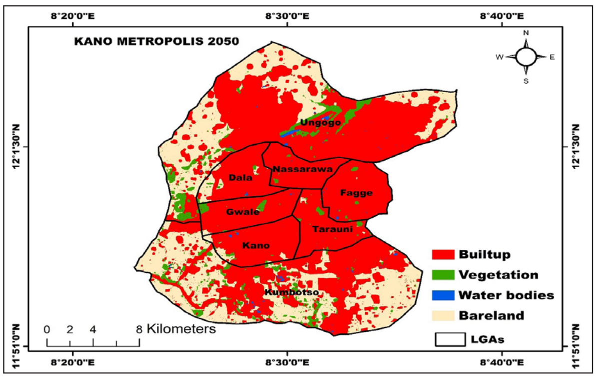


**Figure 7.** LULC map of 2050

### *3.3 LULC statistics*

In 1984, the study area comprised 25.43 km² (7.2%) of built-up land, 20.46 km² (4%) of vegetation, 1.81 km² (0.4%) of water bodies, and 435.81 km² (88%) of bare land. By 1998, built-up land had increased to 53 km² (10.7%), vegetation expanded to 40 km² (8.1%), while water bodies and bare land covered 0.35 km² (0.1%) and 400 km² (81.1%), respectively. By 2023, the built-up area had significantly expanded to 240.06 km² (49%), while vegetation decreased to 29.01 km² (6%). Water bodies remained relatively stable at 0.94 km² (0.4%), whereas bare land declined to 222.46 km² (45%) (Table 6).

Using classified LULC maps of the Kano metropolis from 1984 to 2023, the city's land use was projected for 2050. According to the projections, by 2050, Kano's built-up areas are expected to cover approximately 322.95 km², representing 65% of the city's total landmass. Vegetation areas are projected to cover approximately 24.31 km², accounting for 5% of the city's total landmass. Water bodies are projected to cover approximately 1.88 km², making up 0.4% of the city's total landmass. Finally, bare land areas are projected to cover approximately 144.33 km², representing 29% of the city's total landmass. (Table 6).

**Table 6**. LULC statistics for 1984, 1998, 2023, and 2050

| LULC Class | 1984 | | 1998 | | 2023 | | 2050 | |
|---|---|---|---|---|---|---|---|---|
| | Area (Km²) | Area (%) | Area (Km²) | Area (%) | Area (Km²) | Area (%) | Area (Km²) | Area (%) |
| Built-up | 35.43 | 7.2 | 53 | 10.7 | 240.06 | 49 | 322.95 | 65 |
| Vegetation | 20.46 | 4 | 40 | 8.1 | 29.01 | 6 | 24.31 | 5 |
| Water bodies | 1.81 | 0.4 | 0.35 | 0.1 | 1.94 | 0.4 | 1.88 | 0.4 |
| Bareland | 435.81 | 88 | 400 | 81.1 | 222.46 | 45 | 144.33 | 29 |
| TOTAL | 493.5 | 100 | 493.5 | 100 | 493.5 | 100 | 493.5 | 100 |

### *3.4 LULC Net change*

Table 7 presents comprehensive LULC change statistics from 1984 - 2023 and projections from 2023-2050. The results indicate that between 1984 and 2023, the built-up area increased by 204.63 km² (41.8%). Vegetation expanded by 8.55 km² (2%). Water bodies experienced a slight decrease of 0.12 km² (0%), while bare land decreased by 43%. For the period from 2023 to 2050, the built-up area is projected to increase by 82.89 km² (16%), the vegetation area is projected to decrease by 4.7 km² (1%), the water body area is projected to decrease by 0.06 km² (0%), and the bare land area is projected to decrease by 78.13 km² (16%).

Figures 8 and 9 depict the change dynamics of various LULC classes over different periods. For 1984-2023, the LULC classes that increased included built-up areas (BU) and vegetation (V). From 2023-2050, BU will continue to increase, while bare land (BL), water bodies (WB), and vegetation (V) will decrease.

**Table 7**. LULC net change statistics

| LULC Class | 1984 - 2023 | | 2023 - 2050 | |
|---|---|---|---|---|
| | Area (Km²) | Area (%) | Area (Km²) | Area (%) |
| Built-up | 204.63 | 41.8 | 82.89 | 16 |
| Vegetation | 8.55 | 2 | -4.7 | -1 |
| Water bodies | 0.13 | 0 | -0.06 | 0 |
| Bareland | -213.35 | -43 | -78.13 | -16 |

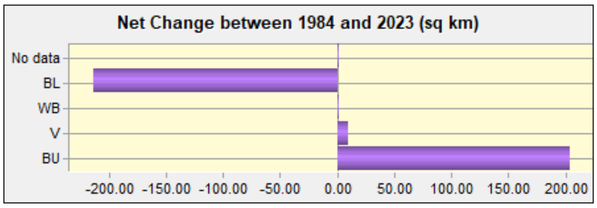


**Figure 8.** Net change from 1984 – 2023

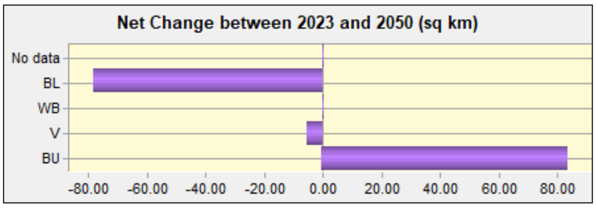


**Figure 9.** Net change from 2023 - 2050

### *3.5 Transition Probability Matrix*

The transition probability matrix (Table 8) illustrates the probability of a specific LULC class transitioning into another land use class. The analysis highlights the built-up areas of the Kano metropolis as the most stable land cover class, with transition probabilities of approximately 0.98. This finding suggests a minimal likelihood of the city's built-up areas transitioning into other LULC categories. Vegetation showed a transition probability of approximately 0.52 for transforming into built-up areas, while water bodies and bare land had transition probabilities of roughly 0.32 for transforming into built-up areas. The analysis (Figure 10) identified bare land and vegetation as the primary LULC classes contributing to the expansion of built-up areas.

**Table 8**. Transition Probability Matrix (1984 – 2023)

| | Built-up | Vegetation | Water bodies | Bareland |
|---|---|---|---|---|
| Built-up | 0.9825 | 0.0058 | 0.0052 | 0.0065 |
| Vegetation | 0.5213 | 0.4336 | 0.0017 | 0.0434 |
| Water bodies | 0.3199 | 0.0373 | 0.3017 | 0.0188 |
| Bareland | 0.3199 | 0.0459 | 0.0027 | 0.6316 |

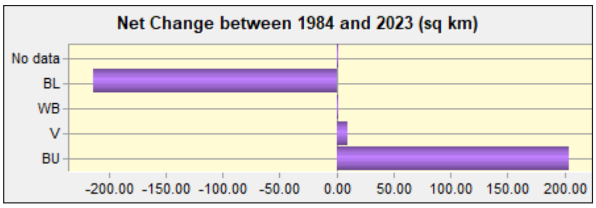


**Figure 10.** LULC classes contributing to changes in built-up areas.

## 4. Discussion

This research reveals that the built-up area will continue to increase at the expense of bare land and vegetation. This finding aligns with the work of Koko et al. (2022), who reported urban growth in the Kano metropolis from 1991 to 2020 at the expense of bare land and vegetation. The rapid urban development of Kano could be attributed to the continuous in-migration of a large population to the city due to various pull factors, including but not limited to suitable farmlands, better business and job opportunities, better urban infrastructure, and healthcare facilities (Koko et al., 2023). Population growth contributes significantly to urban congestion and transforms other land classes into built-up areas (Hussain et al., 2022). The transformation of bare land to built-up areas in the Kano metropolis aligns with a recent study in Delhi that indicated a rapid increase in built-up areas at the expense of bare land (Chaudhuri et al., 2022). A study conducted by Koko et al. (2020) in Zaria and Amaechi et al. (2023) in Abuja, Nigeria, showed that as a result of urbanization and deforestation, these patterns of barren land and vegetation cover turning into built-up areas will persist until 2050. Another study conducted in Bathinda by Rani et al. (2023) suggested that barren land is anticipated to decrease by 2050.

From 1984 to 2023, there was an increase in vegetation cover within the study area. This increase in vegetation could be linked to various Fadama programs (Sulaiman et al., 2021) and government efforts to achieve all-season farming (Koko et al., 2023). A similar increase in vegetation from 1990–2020 was observed in the Zaria metropolis and Abuja Municipal Area Council from 1987–2023 due to afforestation schemes (Koko et al., 2020; Okoduwa et al., 2023). However, the projected results indicate that vegetation will decrease from 2023 to 2050. This decrease in vegetation can be attributed to continuous urbanization and infrastructure development (Amaechi et al., 2023).

Increasing built-up areas at the expense of vegetation cover could jeopardize ecosystem health, human well-being, and food security (Rahman, 2016; Khanal et al., 2019). Gogoi et al. (2019) reported that an increased population could result in increased pollution, leading to detrimental consequences, including urban heat waves and health problems (Hansen et al., 2013; Wang et al., 2021). Okoduwa et al. (2023) confirmed that the increase or decrease in temperature changes was linked to the amount of vegetation cover in cities. It is generally proven that the loss of forest and vegetative cover degrades ecosystem services by reducing water retention, drying up water sources, decreasing biodiversity, reducing the sequestration rate of carbon dioxide ($CO_2$), and enhancing the magnitude and frequency of disasters such as flooding (Bradshaw et al., 2007), which are vital for human well-being (Bewket, 2002).

Urbanization poses challenges to environmental sustainability (Keshtkar et al., 2017; Rijal et al., 2018), as urban expansion often comes at the expense of biodiversity and ecosystem services (Poppenborg and Koellner, 2013; Tao et al., 2015). With urban development, there is a high demand for natural resources (Balatsky et al., 2015), food, and fibre production (Tilman et al., 2011). Consequently, ecosystems face unprecedented pressure, potentially leading to degradation and conversion, thereby affecting the provisioning of ecosystem services for both current and future generations (Rimal et al., 2019). The increase in built-up areas due to urbanization can exacerbate runoff by limiting the areas where floodwaters can flow, as a large part of urban environments are covered with tarred roads and pavement (Mukhtar et al., 2022).

A balance between urban development and the conservation of natural resources is crucial for sustainable urban development (Koko et al., 2022). Implementing strategies such as open green spaces, green infrastructure, water conservation techniques, and various afforestation initiatives is essential for promoting public health and environmental sustainability in urban areas (Okoduwa et al., 2023). These interventions play a critical role in mitigating soil erosion, preventing land degradation, minimizing environmental pollution, and regulating surface temperatures (Tsegaye, 2019; Asuquo et al., 2022). Another way to promote urban sustainability is through developing and implementing a land-use plan (Qingsong He, 2023) that prioritizes sustainable development and protects ecologically valuable areas such as green spaces to mitigate urban heat islands and floods.

## 5. Conclusions and recommendations

To design future policies and plans for healthy urban development, it is vital to understand how LULC has evolved in the past, present, and future. The findings of this study will help policymakers, environmental managers, and individuals improve environmental management methods in the Kano metropolis. To protect vegetation, this study advises the development and implementation of ecosystem-based adaptation strategies and other legal frameworks. Such initiatives should concentrate on planting trees in urban areas such as parking lots, between buildings, in backyards, and along roadways. These steps will considerably protect soil from erosion, support biodiversity, and manage temperature and pollution. To prevent any irreparable effects that changes in LULC may have on the environment in the near future, we urge environmental managers to make use of the conclusions and suggestions of this study.

## References

Alqahtany, A., Rezgui, Y., Lic, H. (2013). A proposed model for sustainable urban planning development for environmentally friendly communities. Architectural Engineering and Design Management 9 (3): 176-194.

Amaechi, C.F., Ugwu, V.C., Okoduwa, A.K. (2024). Geospatial Assessment of Land Use/Land Cover of the Federal Capital Territory: A Case Study For The Year 2050. Ethiopian Journal of Environmental Studies & Management 17 (1): 95 – 109.

Balatsky, A. V., Balatsky, G. I., Borysov, S. S. (2015). Resource demand growth and sustainability due to increased world consumption. Sustainability 7 (3): 3430-3440.

Barau, A. S., Maconachie, R., Ludin, A. N. M., Abdulhamid, A. (2015). Urban morphology dynamics and environmental change in Kano, Nigeria. Land Use Policy 42: 307-317.

Bewket, W. (2002). Land cover dynamics since the 1950s in Chemoga watershed, Blue Nile basin, Ethiopia. Mountain research and development 22 (3): 263-269.

Bradshaw, C. J., Sodhi, N. S., Peh, K. S. H., Brook, B. W. (2007). Global evidence that deforestation amplifies flood risk and severity in the developing world. Global change biology 13(11): 2379-2395.

Bren d'Amour, C., Reitsma, F., Baiocchi, G., Barthel, S., Güneralp, B., Erb, K. H., Seto, K. C. (2017). Future urban land expansion and implications for global croplands. Proceedings of the National Academy of Sciences 114(34): 8939-8944.

Chaudhuri, G., Mainali, K. P., Mishra, N. B. (2022). Analysing the dynamics of urbanization in Delhi National Capital Region in India using satellite image time-series analysis. Environment and Planning B: Urban Analytics and City Science 49 (1): 368-384.

Chotchaiwong, P., and Wijitkosum, S. (2019). Predicting urban expansion and urban land use changes in Nakhon Ratchasima City using a CA-Markov model under two different scenarios. Land 8(9): 140.

Dankani, I. M. (2013). Constraints to sustainable physical planning in Metropolitan Kano. International Journal of Management and Social Sciences Research.

Enoh, M. A., Njoku, R. E., Okeke, U. C. (2023). Modelling and mapping the spatial–temporal changes in land use and land cover in Lagos: A dynamics for building a sustainable urban city. Advances in Space Research 72(3): 694-710.

Fabolude, G., and Aighewi, I.T. (2022). Evaluation of the Extent of Land Use-Land Cover Changes of Benin City, Edo State, Nigeria from 1987-2019. Journal of Applied Science and Environmental Management 26 (8): 1443 - 1450.

Ghalehteimouri, K. J., Shamsoddini, A., Mousavi, M. N., Ros, F. B. C., Khedmatzadeh, A. (2022). Predicting spatial and decadal of land use and land cover change using integrated cellular automata Markov chain model based scenarios (2019–2049) Zarriné-Rūd River Basin in Iran. Environmental Challenges 6: 100399.

Gogoi, P. P., Vinoj, V., Swain, D., Roberts, G., Dash, J., Tripathy, S. (2019). Land use and land cover change effect on surface temperature over Eastern India. ScientificRreports 9(1): 8859.

Guan, D., Gao, W., Watari, K.; Fukahori, H. (2008). Land use change of Kitakyushu based on landscape ecology and Markov model. Journal of Geographical Sciences 18 (4): 455-468.

Han, H., Yang, C., Song, J. (2015). Scenario simulation and the prediction of land use and land cover change in Beijing, China. Sustainability 7(4): 4260-4279.

Hansen, M. C., Potapov, P. V., Moore, R., Hancher, M., Turubanova, S. A., Tyukavina, A., Townshend, J. R. (2013). High-resolution global maps of 21st-century forest cover change. Science 342(6160): 850-853.

He, C., Shi, P., Chen, J., Li, X., Pan, Y., Li, J., Li, J. (2005). Developing land use scenario dynamics model by the integration of system dynamics model and cellular automata model. Science in China Series D: Earth Sciences 48: 1979-1989.

He, Q. (2023). Urban Planning and Sustainable Land Use. Sustainability 15(12): 9524.

Huang, Q., Huang, J., & Yang, X. (2019). Quantifying the seasonal contribution of coupling urban land use types on Urban Heat Island using Land Contribution Index: A case study in Wuhan, China. Sustainable Cities and Society 44: 666-675.

Hussain, S., Mubeen, M., Karuppannan, S. (2022). Land use and land cover (LULC) change analysis using TM, ETM+ and OLI Landsat images in district of Okara, Punjab, Pakistan. Physics and Chemistry of the Earth, Parts a/b/c 126: 103117.

Jiansheng, W., Zhe, F.E.N.G., Yang, G.A.O., Xiulan, H.U.A.N.G., Hongmeng, L.I.U., Li, H.U.A.N.G. (2012). Recent progress on the application and improvement of the CLUE-S model. Progress in Geography 1: 3-10.

Kadri, N., Jebari, S., Augusseau, X., Mahdhi, N., Lestrelin, G., Berndtsson, R. (2023). Analysis of four decades of land use and land cover change in semiarid Tunisia using Google Earth Engine. Remote Sensing 15 (13): 3257.

Keshtkar, H., Voigt, W., Alizadeh, E. (2017). Land-cover classification and analysis of change using machine-learning classifiers and multitemporal remote sensing imagery. Arabian Journal of Geosciences 10: 1-15.

Khanal, N., Uddin, K., Matin, M. A., Tenneson, K. (2019). Automatic detection of spatiotemporal urban expansion patterns by fusing OSM and Landsat data in Kathmandu. Remote Sensing 11(19): 2296.

Khawaldah, H.A. (2016). A prediction of future land use/ land cover in Amman area using GIS-based Markov Model and remote sensing. International Journal of Geographical Information Science 8(03): 412-427.

Koko, A. F., Bello, M., Sadiq, M. A. (2023). Understanding the Challenges of 21st Century Urbanization in Northern 'Nigeria's Largest City, Kano.

Koko, A. F., Han, Z., Wu, Y., Abubakar, G. A., Bello, M. (2022). Spatiotemporal land use/land cover mapping and prediction based on hybrid modeling approach: a case study of Kano Metropolis, Nigeria (2020–2050). Remote Sensing 14 (23): 6083.

Koko, A. F., Yue, W., Abubakar, G. A., Hamed, R., Alabsi, A. A. N. (2020). Monitoring and predicting spatiotemporal land use/land cover changes in Zaria City, Nigeria, through an integrated cellular automata and markov chain model (CA-Markov). Sustainability 12 (24): 10452.

Li, G., Zhang, X., Mirzaei, P., Zhang, J., Zhao, Z. (2018). Urban heat island effect of a typical valley city in China: Responds to global warming and rapid urbanization. Sustainable Cities and Society 8: 736–745.

Li, J., Li, C., Zhu , F., Song, C., Wu, J. (2013). Spatiotemporal pattern of urbanization in Shanghai, China between 1989 and 2005. Landscape Ecology 28: 1545–1565.

Lia, J., Oyanaa, T., Mukwayac, P. (2016). An examination of historical and future land use changes in Uganda using change detection methods and agent-based modeling. African Geographical Review 35(3): 247–271.

Liang, X., Zeng, G., Yujie, Y. (2019). The effects of interaction between climate change and landuse/cover change on biodiversity-related ecosystem services. Global Challenges 3: 1-8.

Liping, C., Yujun, S., Saeed, S. (2018). Monitoring and predicting land use and land cover changes using remote sensing and GIS techniques—A case study of a hilly area, Jiangle, China. PloS one 13 (7): e0200493.

Mohamed, M. A., Anders, J., Schneider, C. (2020). Monitoring of changes in land use/land cover in Syria from 2010 to 2018 using multitemporal Landsat imagery and GIS. Land 9 (7): 226.

Mohammed, M. U., Musa, I. J., Jeb, D. N. (2014). GIS-based analysis of the location of filling stations in metropolitan Kano against the physical planning standards. American Journal of Engineering Research 3 (9): 147-158.

Mukhtar, I., Iguisi, E. O., Shehu, A. U., Dabo, Y., Abubakar, M., Zubairu, S. M., Balarabe, A. (2020). Effects of Landuse and Landcover Change on Flooding in Kano Metropolis, Kano State, Nigeria. Fudma Journal of Sciences 4 (3): 505-512.

Nabegu, A. B. (2014). Analysis of vulnerability to flood disaster in Kano State, Nigeria. Greener journal of physical sciences 4 (2): 22-29.

Nasiri, V., Deljouei, A., Moradi, F., Sadeghi, S.M.M., Borz, S.A. (2022). Land use and land cover mapping using Sentinel-2, Landsat-8 Satellite Images, and Google Earth Engine: A comparison of two composition methods. Remote Sensing 14 (9): 1977.

Nourqolipour, R., Mohamed Shariff , A. B., Balasundram, S., Ahmad , N., Sood , A., Buyong, T. (2016). Predicting the effects of urban development on land transition and spatial patterns of land use in Western Peninsular Malaysia. Applied Spatial Analysis and Policy 9 (1), 1-19.

Nwagbara, M. O. (2015). Case study: Emerging advantages of climate change for agriculture in Kano State, northwestern Nigeria. American Journal of Climate Change 4 (3): 263-268.

Okoduwa, A., and Amaechi, C. F. (2024). Exploring Google Earth Engine, Machine Learning, and GIS for Land Use Land Cover Change Detection in the Federal Capital Territory, Abuja, between 2014 and 2023. Applied Environmental Research 46 (2).

Okoduwa, K. A., Amaechi, C.F., Enuneku, A. A. (2024) Soil Adjusted Vegetation Index, Normalized Difference Buildup Index, and Land Surface Temperature between 1987 and 2023 in Abuja Municipal Area Council, Nigeria. Journal of Applied Science and Environmental Management 28 (3): 665-674.

Okopi, M. (2021). Urbanization and sustainable growth of urban Kano, Nigeria. In IOP Conference Series: Earth and Environmental Science. IOP Publishing, 1(665):012063

Osman, T., Shawb, D., Kenawy, E. (2018). An integrated land use change model to simulate and predict the future of greater Cairo metropolitan region. Journal of Land Use Science 13(6): 565– 584.

Rahman, M. T. (2016). Detection of land use/land cover changes and urban sprawl in Al-Khobar, Saudi Arabia: An analysis of multitemporal remote sensing data. ISPRS International Journal of Geo-Information 5 (2): 15.

Rahnama, M. R. (2021). Forecasting land-use changes in Mashhad Metropolitan area using Cellular Automata and Markov chain model for 2016-2030. Sustainable Cities and Society 64: 102548.

Rani, A., Gupta, S. K., Singh, S. K., Meraj, G., Kumar, P., Kanga, S., Dogančić, D. (2023). Predicting future land use utilizing economic and land surface parameters with ANN and Markov chain models. Earth 4(3): 728-751.

Rigden, A., and Li, D. (2017). Attribution of surface temperature anomalies induced by land use and land cover changes. Geosphacial Research Letters, 44(13): 6814-6822.

Rimal, B., Sharma, R., Kunwar, R., Keshtkar, H., Stork, N. E., Rijal, S., Baral, H. (2019). Effects of land use and land cover change on ecosystem services in the Koshi River Basin, Eastern Nepal. Ecosystem services 38: 100963.

Rimal, B., Zhang, L., Keshtkar, H., Sun, X., Rijal, S. (2018). Quantifying the spatiotemporal pattern of urban expansion and hazard and risk area identification in the Kaski District of Nepal. Land 7(1): 37.

Samat, N., Mahamud, M. A., Tan, M. L., Maghsoodi Tilaki, M. J., Tew, Y. L. (2020). Modeling land cover changes in peri-urban areas: A case study of George Town conurbation, Malaysia. Land 9(10): 373.

Simwanda, M., and Murayama, Y. (2018). Spatiotemporal patterns of urban land use change in the rapidly growing city of Lusaka, Zambia: Implications for sustainable urban development. Sustainable Cities and Society 39: 262–274.

Singh, P., Kikon, N., VermaAmity, P. (2017). Impact of land use change and urbanization on urban heat island in Lucknow city, Central India. A remote sensing based estimate. Sustainable Cities and Society 32: 100-114.

Sulaiman, S. M., Yahaya, A., Muhammad, M. A., Muhammad, A. D. (2021). Evaluating Fadama III Development Project in Kano State, Nigeria: Using Difference in Difference Estimation with Propensity Score Matching Approach. International Journal of Economics, Management and Accounting 499-517.

Sun, X., Crittenden, J. C., Li, F., Lu, Z., Dou, X. (2018). Urban expansion simulation and the spatiotemporal changes of ecosystem services, a case study in Atlanta Metropolitan area, USA. Science of the Total Environment 622, 974-987.

Tilman, D., Balzer, C., Hill, J., Befort, B. L. (2011). Global food demand and the sustainable intensification of agriculture. Proceedings of the national academy of sciences 108(50): 20260-20264.

Tobore, A., Senjobi, B., Oyerinde, G. (2021). Spatio Temporal Analysis and Simulation Pattern of Land Use and Land Cover Change in Odeda Peri-urban of Ogun State, Nigeria. Jordan Journal of Earth & Environmental Sciences 12(4).

Tsegaye, B. (2019). Effect of land use and land cover changes on soil erosion in Ethiopia. International Journal of Agricultural Science and Food Technology 5(1): 26-34.

United Nations Department of Economic and Social Affairs. World Urbanization Prospects: The 2018 Revision. Available online: https://population.un.org/wup/Country-Profiles/ (accessed on 15 June 2020).

Verburg, P. H., and Overmars, K. P. (2007). Dynamic simulation of land-use change trajectories with the CLUE-s model. Modelling land-use change: Progress and applications 321-337.

Wang, K., Zhang, J., Huang, H. (2019, June). Impact of Land Use/cover Changes on Carbon Storage in Chinese Resource-Based City. In Abstract Proceedings of 2019 International Conference on Resource Sustainability-Cities (icRS Cities).

Wang, R., Hou, H., Murayama, Y. (2018). Scenario-based simulation of Tianjin City using a cellular automata–Markov model. Sustainability 10 (8): 2633.

Wang, S. W., Munkhnasan, L., Lee, W. K. (2021). Land use and land cover change detection and prediction in Bhutan's high altitude city of Thimphu, using cellular automata and Markov chain. Environmental Challenges 2: 100017.

Wang, S., and Zheng, X. (2023). Dominant transition probability: Combining CA-Markov model to simulate land use change. Environment, Development and Sustainability 25(7): 6829-6847.

Xu, C., Liu, M., Hong, C., Chi, T. (2012). Temporal variation of characteristic scales in urban landscapes: an insight into the evolving internal structures of 'China's two largest cities. Landscape Ecology 27: 1063–1074.

Yuan, T., Yiping, X., Lei, Z., Danqing, L. (2015). Land use and cover change simulation and prediction in Hangzhou city based on CA-Markov model. International Proceedings of Chemical. Journal of Biological and Environmental Engineering 90: 108-113.

Zhu, X., Zhang, P., Wei, Y., Li, Y., Zhao, H. (2019). Measuring the efficiency and driving factors of urban land use based on the DEA method and the PLS-SEM—A case study of 35 large andmedium-sized cities in China. Sustainable Cities and Society 50:101646.